

Spectral random walks and line broadening of impurity molecules in an Ising spin glass environment

Yoshitaka Tanimura

Institute for Molecular Science, Myodaiji, Okazaki, Aichi 444, Japan

Hiroshi Takano

Department of Physics, Keio University, Hiyoshi, Yokohama 223, Japan

Joseph Klafter

School of Chemistry, Tel-Aviv University, 69978 Tel-Aviv, Israel

(Received 15 July 1997; accepted 24 October 1997)

Transition energy fluctuations in impurity molecules, embedded in an inhomogeneous environment, are investigated within an Ising spin model of the environment. The spatially distributed impurity molecules are assumed to interact with the Ising spin glass through dipole–dipole type of interaction. We calculate the fluctuations in the transition energies of impurity molecules, for different temperatures and various Ising parameters, and find that the spectral distribution of the fluctuations follows approximately a $1/f$ power law. The fluorescence spectra of the impurity molecules yield microscopic information about domain structures in the Ising environment. In the case of large disorder, the distribution of transition energies shows profiles similar to those observed in single molecule spectroscopy. © 1998 American Institute of Physics. [S0021-9606(98)51405-5]

I. INTRODUCTION

The use of nonlinear optical field interactions to probe the properties of matter has been propelled by the rapid advances in laser measurement techniques. Recently, the ultimate limit of optical spectroscopy, single molecule detection (SMD), has been attained, in which the spectral properties of individual single impurity molecules in solids,^{1–7} polymers,^{8,9} liquids,^{10–18} and on surfaces^{19–22} are measured, with the ensemble average removed. The SMD technique provides information about the nature of the homogeneous lineshape, which is often obscured by inhomogeneous broadening. One is able now to study the line shapes and linewidths of single molecules and their modification by the environment, the temperature, or by the applied laser fields, and thus gain information about the molecules themselves and their local environment.

An observable which has recently drawn attention in spectroscopic studies of single impurity molecules in host systems is the modulation with time of their transition energies. In many cases, these energy modulations are assumed, to a good approximation, to have a Gaussian nature. This is obviously true if the interactions between the impurities and host have a cumulative effect of a large number of weak interactions, and the regular central limit theorem comes into play. This allows, for instance, to use an ensemble of harmonic oscillators as the host system, which leads to a Gaussian modulation of the impurity molecules. One should notice, however, that the Gaussian nature of the modulations does not mean that all individual modulations follow a Gaussian. The ability to measure transition energies of single molecules opens the possibility to measure non-Gaussian characteristics of single modulations directly from experiments, as was pointed out by Wang and Wolynes.²³

Here, we present a simple theoretical model which ad-

dresses the problem of the transition energy fluctuations of single molecules embedded in a matrix, emphasizing the dependence on temperature and on disorder. The energy fluctuations, which appear as spectral noise, can be described in terms as spectral random walks.^{1,24–31} The assumptions in our model have been partly motivated by the experimental observations in system of dilute pentacene doping of *p*-terphenyl crystals. The *p*-terphenyl molecule consists of three phenyl rings and, in the crystalline phase, the two outer rings lie in the same plane, whereas the central ring can twist either clockwise or anticlockwise relative to this plane.³² Above a critical temperature ($T=193$ K), the motion of the central phenyl ring corresponds to motion in a symmetric double well potential, and the two possible configurations of central ring occur equally. Below the critical temperature, however, interactions between neighboring *p*-terphenyl molecules lead to an asymmetric double well potential for the central ring motion, and the central phenyl rings are antiferromagnetically ordered.³³ Due to thermal excitations, associated with some defects in the crystal, the central ring can flip even well below the critical temperature. The spectral noise of the pentacene impurity is believed to measure the fluctuations of the terphenyl environment. Such systems have been studied theoretically using randomly distributed, independent, two-level systems (TLS),^{30,34,24} which follow the Anderson–Kubo processes.³⁵ In the model, the TLSs correspond to the two lowest quantum states associated with reorientation of the central phenyl ring of *p*-terphenyl. Our approach is to introduce the Ising spin glass model, whose properties have been extensively studied within the field of critical phenomena,^{36,37} as the host lattice. The Ising spin model introduces coupling between the spins which represent the dynamical environment, an aspect missing in the conventional TLS model. Depending on the choice of parameters, this model yields an inhomogeneous structure of do-

mains, due to frustration in the bond configurations. Near the domain boundaries the Ising spins can flip even at low temperatures. In the current model, the domains which determine the spectral noise of the impurity molecules, are controlled by the bond distributions and initial conditions, whereas, in the TLS model, the neighboring structures around impurities are assumed from the start to be randomly distributed TLS. Our aim is to embed impurity molecules into the host Ising spin glass system and probe the local flips of the spins by following the changes in the transition frequencies of the impurity molecules. We investigate the statistical properties of the fluctuations (spectral noise) averaged over time, or ensemble, and calculate power spectra and line broadening. The present model is probably too idealized to discuss dynamics in pentacene doped terphenyl crystals. However, it does capture some general properties of molecules interacting with a frustrated environment. This can be extended to other systems, such as solvent molecules in water, where the water is simulated by the spin glass system as has been proposed in Refs. 38–43. Our approach combines the knowledge of spin glasses, heat-baths, and fluctuation analysis to study molecular spectroscopy in condensed phases.

In Sec. II we outline the model of impurity molecules coupled to an Ising spin glass environment. The basic steps of the Monte Carlo simulation are also explained. In Sec. III we present results of simulations for various initial conditions, bond configurations, and coupling strengths. We end with a summary in Sec. IV.

II. IMPURITY MOLECULES IN ISING SPIN GLASS ENVIRONMENT

We consider impurity molecules embedded in a disordered environment modeled by the kinetic Ising model. We first describe the environment itself, and then introduce impurity molecules whose spectral noise we follow.

Let us consider a system of N Ising spins in a lattice with a quenched bond disorder. The Hamiltonian of the system, including the factor $-1/(k_B T)$, where k_B and T are the Boltzmann constant and the temperature, respectively, is given by

$$\mathcal{H}_B = -\frac{1}{k_B T} H_B = \frac{1}{k_B T} \sum_{\langle i,j \rangle} J_{ij} S_i S_j = \sum_{\langle i,j \rangle} K_{ij} S_i S_j. \quad (2.1)$$

Here, $S_i = \pm 1$ denotes an Ising spin at the i th site, and $\sum_{\langle i,j \rangle}$ denotes summation over all the nearest-neighbor pairs. Each coupling constant K_{ij} is an independent quenched random variable. In the case of the $\pm J$ Ising model, K_{ij} is equal to $K > 0$ with probability p , or $-K$ with probability $1-p$.

The dynamics of the system is assumed to be described by the single-spin-flip kinetic Ising model.^{44–46} The probability $P(S;t)$ that the system has a spin configuration $S = (S_1, S_2, \dots, S_N)$ at time t obeys the master equation

$$\frac{\partial}{\partial t} P(S;t) = \sum_i [-W_i(S)P(S;t) + W_i(F_i S)P(F_i S;t)], \quad (2.2)$$

where $F_i S$ denotes a spin configuration obtained from S by flipping the i th spin: $F_i S = (S_1, \dots, -S_i, \dots, S_N)$ for $S = (S_1, \dots, S_i, \dots, S_N)$. The transition probability per unit time, $W_i(S)$, for the i th spin to flip in a configuration S is chosen to be of the Glauber type,^{44–46}

$$W_i(S) = \frac{1}{2\tau} (1 - S_i \tanh E_i) \quad (2.3)$$

with

$$E_i = \sum_j \langle i \rangle K_{ij} S_j, \quad (2.4)$$

where $\sum_j \langle i \rangle$ denotes summation over all nearest-neighbor sites of the i th site, and τ represents the time scale for a noninteracting spin to flip. It should be noted that this transition probability satisfies the detailed balance condition

$$W_i(S)P_{\text{eq}}(S) = W_i(F_i S)P_{\text{eq}}(F_i S), \quad (2.5)$$

where

$$P_{\text{eq}}(S) \propto \exp[\mathcal{H}_B(S)] \quad (2.6)$$

is the equilibrium distribution.

In this paper, a standard Monte Carlo method, which uses discrete time steps and updates spins in a random sequence, is applied to generate a sample of the time evolution of spin configurations, described by the master equation (2.2). (i) We start by specifying an initial condition for the set of $\{S_i\}$. (ii) We select one spin configuration (S_i) in which one dynamical variable will be changed randomly from S_i to S'_i . The index i is selected by going through the array of spin labels randomly. (iii) We compute the change in energy E_i , produced by the trial move, using Eq. (2.4), and the transition probability $W_i(S)$ using Eq. (2.3). (iv) We select a random number z in the interval $0 < z < 1$. (v) If $\tau W_i > z$ the move is accepted, i.e., S_i is replaced by S'_i ; otherwise the move is rejected, i.e., the state with the previous configuration (S_i) is counted once more as a “new” state. The time τ/N in the master equation (2.2) corresponds to procedures (ii)–(v). (vi) We repeat procedures (ii)–(v) N times, which defines one Monte Carlo step (MCS). One can set τ to unity so that the unit time of the master equation agrees with one Monte Carlo step. Although there are other algorithms for generating sample paths, this procedure describes well the dynamics of the Ising environments.

We now introduce impurity molecules into the Ising environment. For simplicity, we assume that the configurations of the Ising system are not modified by the impurities. In addition, we assume that the spins and impurities share the same lattice sites, and that the impurities do not perturb the dynamics of the spin system. This is a rather unrealistic assumption, since impurity molecules most likely introduce some defects into the crystal structure, such as deformations of bond configurations or dislocations of spin (terphenyl) molecules. It is not difficult to incorporate such effects into model; however, here we consider the simplest case as a starting point.

We assume that the impurity molecules interact via dipole–dipole type interaction with the surrounding spins. Namely, the coupling between the molecules and spins depends on the distance as^{47,48}

$$w(\mathbf{r}_{ij}) = \frac{\Psi(\Omega_{ij})}{r_{ij}^3}, \quad (2.7)$$

where r_{ij} is the distance between the i th impurity and the j th spin, and $\Psi(\Omega_{ij})$ is a function of the polar angle Ω_{ij} . $\Psi(\Omega_{ij})$ is assumed to be one for 2D Ising model. The transition frequency at site i is denoted by $\omega_i(t)$ and can be calculated according to

$$\omega_i(t) = \omega_0 + \sum_{j \neq i} w(\mathbf{r}_{ij}) S_j(t), \quad (2.8)$$

where ω_0 is the transition frequency of the bare impurity molecule itself and is set equal to zero. The transition frequency $\omega_i(t)$ in Eq. (2.8) carries information about the surrounding environment. Until recently, one could only measure ensembles of impurity molecules and therefore obtain inhomogeneously broadened spectra. The ability to measure transition energies of single molecules makes it possible to investigate the individual time series $\omega_i(t)$. In the next section, we carry out numerical simulation of the model to demonstrate the characteristics of the spectral random walks of single molecules, emphasizing the dependence on the embedding host system and on temperature.

III. NUMERICAL RESULTS AND DISCUSSION

The $\pm J$ Ising model in the case of the simple cubic lattice has a paramagnetic phase, a ferromagnetic phase, an antiferromagnetic phase, and a spin glass phase. These phases are described by the magnetization $m = \sum_i \langle S_i \rangle / N$, the staggered magnetization $m_s = (\sum_{i \in A} \langle S_i \rangle - \sum_{i \in B} \langle S_i \rangle) / N$ and the Edwards–Anderson spin glass order parameter⁴⁹ $q = \sum_i \langle S_i \rangle^2 / N$. Here, the lattice is divided into two interpenetrating sublattices A and B in such a way that no nearest-neighbor pair of sites belongs to the same sublattice. Summation over all sites on the A sublattice and that on the B sublattice are denoted by $\sum_{i \in A}$ and $\sum_{i \in B}$, respectively. In the paramagnetic phase, $m = m_s = q = 0$; in the ferromagnetic phase, $m \neq 0$ and $m_s = 0$; in the antiferromagnetic phase, $m = 0$ and $m_s \neq 0$; in the spin glass phase, $m = m_s = 0$ and $q \neq 0$. Note that $q \neq 0$ if $m \neq 0$ or $m_s \neq 0$.

The phase diagram of the simple cubic lattice^{50,51} is schematically shown in Fig. 1(a). For a fixed p , the system shows a phase transition at $K^{-1} = K_c^{-1}(p)$. In the high temperature regime, $K^{-1} > K_c^{-1}(p)$, the phase is paramagnetic. In the low temperature regime, $K^{-1} < K_c^{-1}(p)$, the phase is ferromagnetic for $p_c < p \leq 1$, it is antiferromagnetic for $0 \leq p < 1 - p_c$, and it is a spin glass phase, for $1 - p_c < p < p_c$. Because of the symmetry of the Hamiltonian (2.1), the transition temperature satisfies $K_c^{-1}(p) = K_c^{-1}(1 - p)$. As p increases, $K_c^{-1}(p)$ decreases for $0 \leq p \leq 0.5$ and increases for $0.5 \leq p \leq 1$. It is continuous at $p = p_c$ and $p = 1 - p_c$; $K_c(p_c + 0) = K_c(p_c - 0)$ and $K_c(1 - p_c + 0) = K_c(1 - p_c - 0)$. The phase boundary between the ferromagnetic and the spin glass

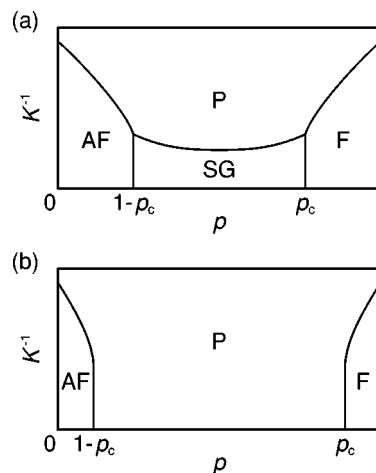


FIG. 1. The phase diagram of the $\pm J$ Ising model for (a) the simple cubic lattice and (b) the square lattice. The paramagnetic, ferromagnetic, antiferromagnetic, and spin glass phases are denoted by P , F , AF , and SG , respectively.

phases is given by $p = p_c$ and $0 \leq K^{-1} \leq K_c^{-1}(p_c)$. In the same way, the phase boundary between the antiferromagnetic and the spin glass phases is given by $p = 1 - p_c$ and $0 \leq K^{-1} \leq K_c^{-1}(1 - p_c)$.

In the case of the $\pm J$ Ising model for the square lattice, the spin glass phase is believed to disappear as shown in Fig. 1(b). Thus, $K_c^{-1}(p) = 0$ for $1 - p_c < p < p_c$, and $K_c^{-1}(p_c + 0) > K_c^{-1}(p_c - 0) = 0$ and $K_c^{-1}(1 - p_c - 0) > K_c^{-1}(1 - p_c + 0) = 0$. The line $p = p_c$ with $0 \leq K^{-1} < K_c^{-1}(p_c + 0)$ is the boundary between the ferromagnetic phase and the paramagnetic phase. The line $p = 1 - p_c$ with $0 \leq K^{-1} < K_c^{-1}(1 - p_c - 0)$ is the boundary between the antiferromagnetic and the paramagnetic phases.

In the $\pm J$ Ising model, the temperature regime $K_c^{-1}(p) < K^{-1} < K_c^{-1}(p = 1)$ for a fixed p , where $m = m_s = q = 0$, is called the Griffiths phase. In the Griffiths phase, the relaxation of the averaged spin autocorrelation function is predicted^{52–56} to be anomalously slow. The prediction is based on the following argument: There exists an arbitrarily large compact cluster of spins which can be regarded as a region equivalent to a ferromagnetic pure system. Below the critical temperature of the pure system, the spins in the cluster relax cooperatively with a very long relaxation time. The independent motion of such clusters dominates the long-time behavior of the system, and gives rise to the anomalously slow relaxation of the averaged spin autocorrelation function.

In the $\pm J$ square lattice Ising model, a unit cell surrounded by an odd number of antiferromagnetic bonds is called a frustrated plaquette. In a frustrated plaquette no spin configuration is energetically preferable for all the four bonds, which means that at least one bond is energetically unsatisfied with any spin configuration. A region without frustrated plaquette is equivalent to a pure system and can be regarded as a cluster in the Griffiths phase mentioned above.^{52–56}

In the following, we employ the $\pm J$ spin glass model as

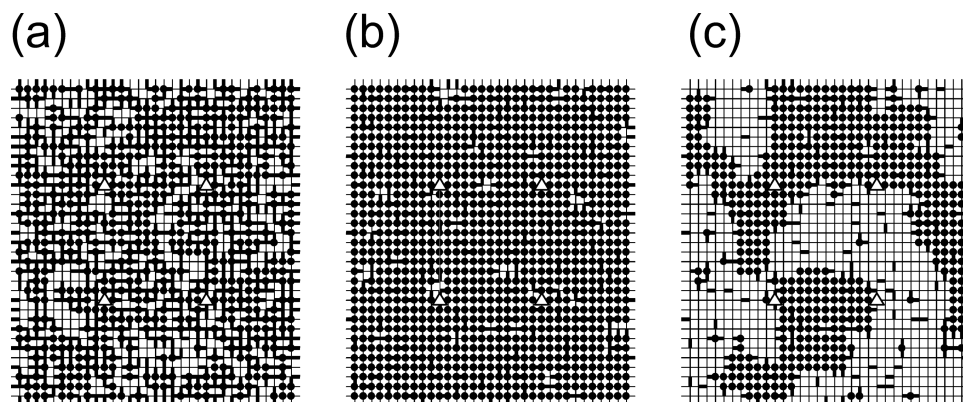


FIG. 2. Bond configuration and equilibrium clusters at a low temperature ($K=4.0$) in two-dimensional spin glass model for cases of (a) a large disorder with a ‘‘half up’’ initial spin configuration ($p=0.5$, $p_s=0.5$); (b) a small disorder with ‘‘all up’’ initial spin configuration ($p=0.9$, $p_s=1.0$); (c) a small disorder with ‘‘half up’’ initial spin configuration ($p=0.9$, $p_s=0.5$). A thin line represents a bond with K , whereas a thick line a bond with $-K$. The sites marked with black circle means spins are in the up state. Transition frequencies of impurity molecules $\omega_i(t)$ are calculated at the sites denoted by the triangles.

a model of a disordered environment. We limit our investigation to the case of the square lattice, which is simpler and which approximates well the anisotropic interactions in *p*-terphenyl crystals.³³ The ‘‘up’’ and ‘‘down’’ spin states correspond to the two lowest quantum states associated with the reorientations of the central phenyl ring of *p*-terphenyl. We believe that, although not completely realistic, this model suffices to capture some general properties of impurity molecules interacting with a frustrated environment, and gives physical insight into the mechanism of broadening.

Monte Carlo simulations were carried out on a 64×64 square lattice with periodic boundary conditions. We denote the bond randomness by p , the bond coupling (inverse temperature) by K , and the probability of ‘‘up’’ spins at the initial configuration by p_s . In our calculations we discarded the initial 10 000 MCS for equilibration.

In the following, we report the results of simulations for parameters $p=0.5$ and 0.9 and $K=0.6$ and 4.0 with $p_s=0.5$ and 1 . Because $K_c^{-1}(p=1) \approx 2.27$, $p_c \approx 0.89$, $K_c^{-1}(p=p_c+0) \approx 0.96$ and $K_c^{-1}(p=0.9) \approx 1.28$,⁵¹ for the square lattice, the case $p=0.9$ with $K=4.0$ corresponds to the ferromagnetic phase and the other cases correspond to the Griffiths phase.

Figures 2 and 3 show spin configurations obtained after discarding 10 000 MCS for 64×64 systems with $K=4.0$ and $K=0.6$, respectively. Only a part of each system (32×32) is shown. The figures also present bond configurations of the systems.

Figure 2(a) corresponds to the case of a large bond disorder ($p=0.5$) with a random initial spin configuration ($p_s=0.5$). As mentioned above, the system with $K=4.0$ at $p=0.5$ is in the Griffiths phase. It can be seen in Fig. 2(a) that spins in each frustration-free region take an energetically preferable configuration, which is the ground state of the region. As explained above, these frustration-free regions correspond to clusters in the Griffiths phase.

Figures 2(b) and 2(c) correspond to the case of small bond disorder ($p=0.9$). The initial configurations for Fig. 2(b) and Fig. 2(c) are ‘‘all up’’ ($p_s=1$) and random (p_s

$=0.5$), respectively. The system with $K=4.0$ at $p=0.9$ is in the ferromagnetic phase. The spin configuration shown in Fig. 2(b) is a typical equilibrium spin configuration, which is the ground state configuration with some thermal fluctuations. In the ground state configuration, almost all spins have the same sign. Because of the existence of antiferromagnetic bonds, some spins should have the opposite sign. The signs of some spins are not determined due to the effects of the frustrated plaquettes. Such spins can fluctuate even at very low temperatures.

In Fig. 2(b), the equilibrium state is obtained after 10 000 MCS of the simulation. This is because the ‘‘all up’’ initial configuration is very close to a ground state configuration. The spin configuration shown in Fig. 2(c) is, in contrast, regarded as a metastable state which appears in the course of the ordering process, starting from the random initial configuration. Such an ordering process occurs as a motion of domain walls, which are boundaries between two ordered regions, with different signs of magnetization. In the

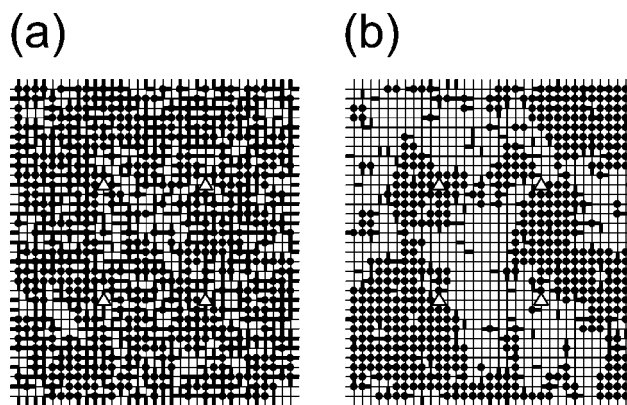


FIG. 3. Bond configuration and equilibrium clusters at a high temperature ($K=0.6$) in a two-dimensional spin glass model for cases of (a) a large disorder with ‘‘half up’’ initial spin configuration ($p=0.5$, $p_s=0.5$); (b) a small disorder with ‘‘all up’’ initial spin configuration ($p=0.9$, $p_s=1.0$). A thin line represents a bond with K , whereas a thick line a bond with $-K$ as symbols in Fig. 2.

case of the pure system ($p=1$), curved domain walls are unstable and the system, which is of finite size, eventually reaches the equilibrium state with no domain walls (or a metastable state with straight domain walls). In the present case, because of the existence of small concentration of antiferromagnetic bonds, the motion of domain walls is considered to be pinned, and a spin configuration with curved domain walls can be metastable with very long lifetime.

Figure 3(a) corresponds to the case of $p=0.5$ and $p_s=0.5$ with $K=0.6$. The system is in the Griffiths phase. In the same way as in Fig. 2(a), spins in each frustration-free region are in an energetically preferable configuration. Because the temperature is higher than in Fig. 2(a), more spins can flip from the energetically preferable configuration than in Fig. 2(a).

Figure 3(b) corresponds to the case of $p=0.9$ and $p_s=1.0$ with $K=0.6$. In contrast to Figs. 2(b) and 2(c), the system in this case is considered to be in the Griffiths phase and spins are found to flip cooperatively as clusters.

The transition frequencies $\omega_i(t)$ were calculated from Eq. (2.8) for the four sites marked in Figs. 2 and 3, respectively, and shown in Figs. 4(a)–8(a). We also calculated the power spectrum for each time series $\omega_i(t)$ according to

$$I_i(\Omega) = \left| \frac{1}{T} \int_0^T dt e^{i\Omega t} \omega_i(t) \right|^2 \quad (3.1)$$

and displayed the results in Figs. 4(b)–8(c) plotted in log–log scale.

Figures 4–6 describe the low temperature case, and correspond to Figs. 2(a), 2(b), and 2(c), respectively. Because of the bond frustration, spins can flip even at this low temperature. Figure 4 is for large bond randomness. The flippings of spins around an impurity molecule induce the spectral jumps in the transition frequency of the impurity. One observes, as seen in Fig. 4(a), small random modulations in the spectral trajectory, which originate from the flippings of spins far from the impurity molecules, superimposed on larger modulations, which originate from the closer spins. However, only a small number of spins can flip at these low temperatures, and the resulting noise shows stepwise fluctuations. Figure 4(b) shows the power spectrum of the noise. The $1/f$ noise character is observed for $f > f_c = 0.03$ – 0.1 , which indicates that the correlation of spin fluctuations decays not as a single process, but through multiple processes which depend on the local spin configuration.

Figure 5 is for small bond randomness. In this case, spins which can flip are associated with the frustrated plaquettes. Since large number of spins hardly change at this low temperature, the characteristic frequency of noise is determined from the dynamics of uncorrelated spins. Thus, the power spectrum of the noise becomes $\propto 1/(f^2 + \tau^{-2})$, where $\tau = 1$, since the noise correlation, in this case, is expressed as $\propto \exp(-t/\tau)$. One should note that if the spins which can flip are subject to a zero local field, and the time scale of the collected motion of spins is much longer than τ , then the dynamics of spins coincided with that of independent TLS.

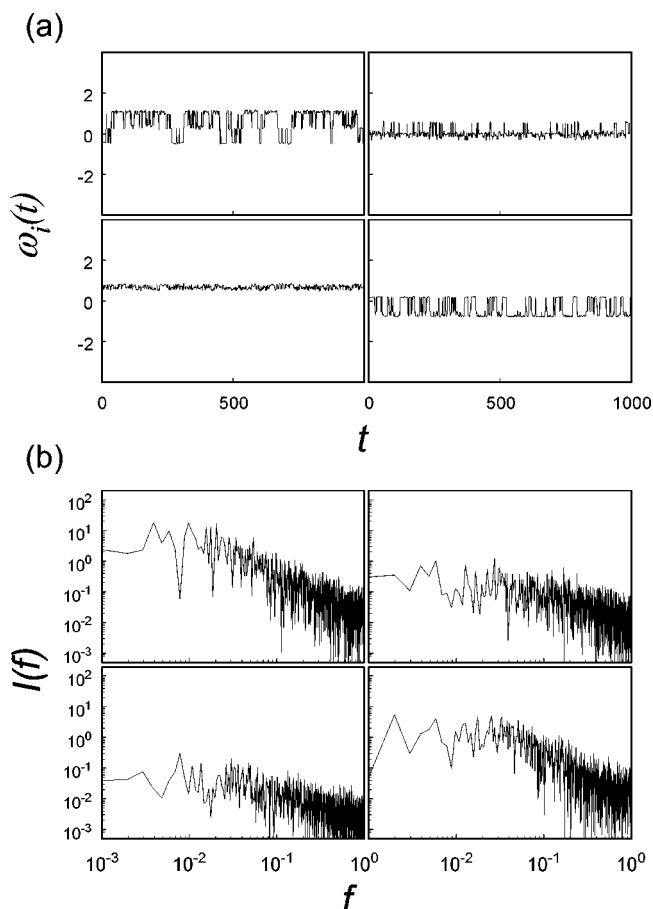


FIG. 4. Transition frequencies of impurity molecules $\omega_i(t)$ and their power spectra (log–log plot) in the case of Fig. 2(a). Each figure is placed in the same order of the impurity molecules denoted in Fig. 2(a).

Figure 6 is again for small bond randomness, but, the initial spin configuration is random ($p_s=0.5$). In this case, the system is not in equilibrium, but in a metastable state with domain walls [Fig. 2(c)]. Each domain wall can fluctuate without an energy change as long as its perimeter does not change. In other words, spin flips can occur along the domain walls. Thus, the flips should have some correlation mediated by the domain walls. Since flips of the spins are correlated, we observe a more pronounced $1/f$ power rule than the case of Fig. 5.

Figures 7 and 8 are for the higher temperature and correspond to Figs. 3(a) and 3(b), respectively. In the case of Fig. 7(a), flippings of spins with various time scales take place throughout the lattice. Thus, the induced spectral noise displays multiscale characteristics with an upper cutoff due to the nearest neighbor restriction. In this case, the ‘‘up’’ and ‘‘down’’ spins are homogeneously distributed and the central frequencies of noises are about $\omega=0$. Figure 7(b) exhibits the power spectrum of the noise. Here, again flippings of spins with various time scales take place throughout the lattice, and the $1/f$ noise character is observed for $f > f_c = 0.03$.

In the case of Fig. 8(a), the flippings occur mainly around a domain. If an impurity molecule is in a domain,

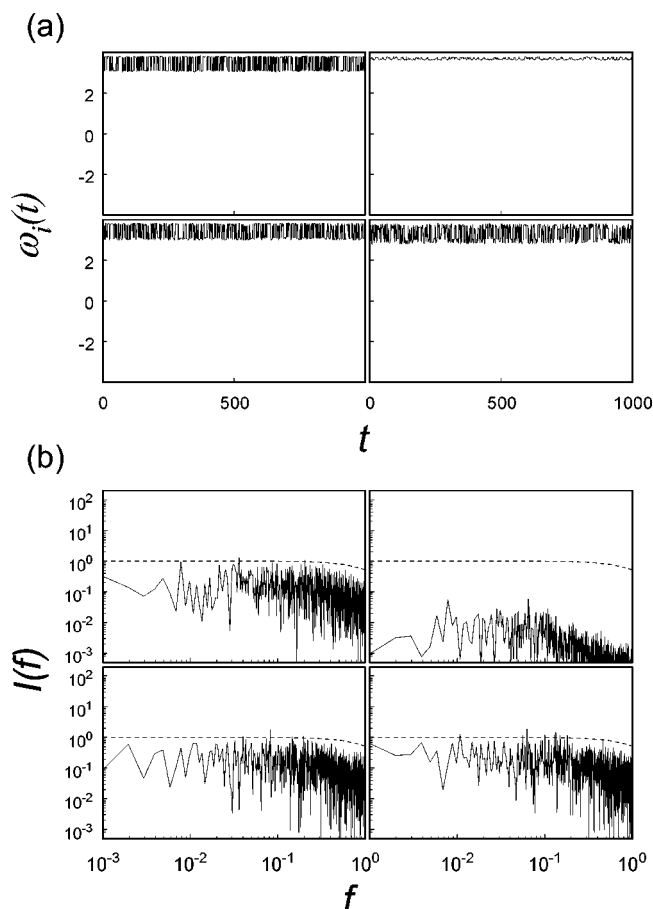


FIG. 5. Transition frequencies of impurity molecules $\omega_i(t)$ and their power spectra (log-log plot) in the case of Fig. 2(b). We plot $I(f) = 1/(f^2 + 1)$ in (b) as a reference. Each figure is placed in the same order of the impurity molecules denoted in Fig. 2(b).

then its noise fluctuates around $\omega = 2$, whereas if it is outside a domain, then it fluctuates around $\omega = -2$. At this temperature, the shape and position of the domain changes rapidly and, following the movement of domain, the central frequency of the spectral noise often jumped between $\omega = 2$ and $\omega = -2$. The power spectra are shown in Fig. 8(b). In each figure, the $1/f$ type spectrum is again observed, however, the lower cutoff, f_c , is shifted to lower frequencies than in the previous case of Fig. 7(b). A possible explanation of this lower values is the formation of domains, which are responsible for slower dynamics observed in Fig. 8(a) as a jump of the central frequency between $\omega = 2$ and $\omega = -2$.

In order to demonstrate the inhomogeneous distribution of impurity molecules, we calculated $\omega_i(t)$ throughout the 64×64 lattice, using Eq. (2.8), and plotted them with a Lorentzian weight,

$$W(\nu) = \sum_i \frac{\gamma}{\gamma^2 + [\nu - \omega_i(t)]^2}. \quad (3.2)$$

This quantity corresponds to the fluorescence (or absorption) spectrum of the impurity molecules and γ corresponds to the natural damping. Note that since we assume that the impurity molecules do not disturb the dynamics of spins, we can eas-

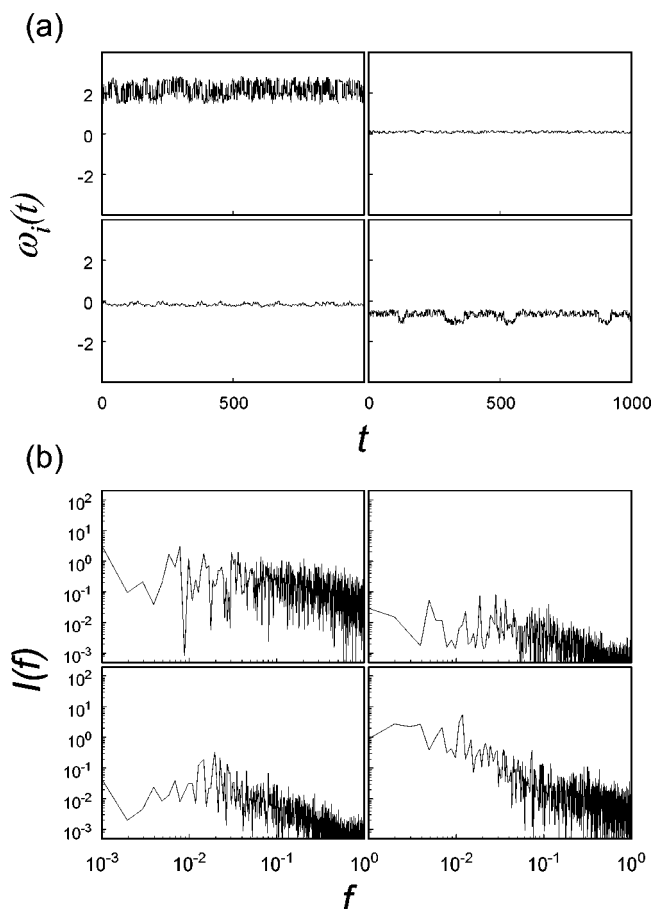


FIG. 6. Transition frequencies of impurity molecules $\omega_i(t)$ and their power spectra (log-log plot) in the case of Fig. 2(c). Each figure is placed in the same order of the impurity molecules denoted in Fig. 2(c).

ily calculate the inhomogeneous distribution. This distribution is constructed from a crude model, which nevertheless gives physical insight into the broadening mechanism.

In Figs. 9 and 10, we present the distribution in each of the cases in Figs. 2 and 3, respectively. Here, we choose $\gamma = 0.02$. In Figs. 9(a) and 10(a) the frequencies are homogeneously distributed and show a similar Gaussian-type distribution. The dynamical properties of each peak are, however, quite different. In the case in Fig. 10(a), each peak fluctuates with large amplitudes, whereas the peaks in Fig. 9(a) stay mostly at the same position, as can be seen from Figs. 4(a) and 7(a).

Figures 9(b) and 10(b) correspond to the case of small bond disorder ($p = 0.9$) with the initial configuration are ‘‘all up’’ ($p_s = 1$). For the lower temperature, Fig. 9(b), the spin system, apart for some thermal fluctuations, is in the ground state configuration where almost all spins have the same sign. Thus, we observe the main peak about $\nu = 3.8$. For the higher temperature, Fig. 10(b), the spins with the same sign form a domain and the distribution of the frequencies is spread. It is clear from Fig. 8(a), that each peak fluctuates more in the higher temperature case, and is more stable in the lower temperature. Figure 9(c) corresponds to the case of small bond disorder ($p = 0.9$) with a random initial configu-

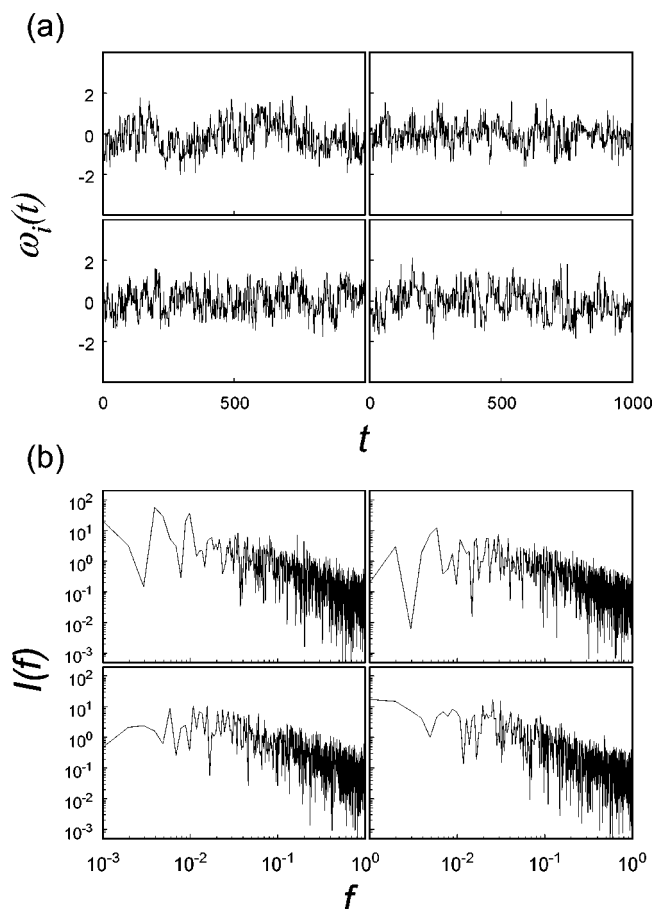


FIG. 7. Transition frequencies of impurity molecules $\omega_i(t)$ and their power spectra (log-log plot) in the case of Fig. 3(a). Each figure is placed in the same order of the impurity molecules denoted in Fig. 3(a).

ration ($p_s=0.5$). As observed in Fig. 2(c), the spins form two types of domains, which are ordered regions with different signs of magnetization. Corresponding to such domain structures the frequencies are widely distributed and show an almost flat distribution. This configuration is considered to be metastable, with a very long lifetime, and is characterized as being almost static.

IV. CONCLUSIONS

We have investigated the effects of environment dynamics on the transition energies of impurity molecules. The environment is modeled by an Ising spin glass. We have carried out Monte Carlo simulation of two-dimensional $\pm J$ spin glass environments for various Ising parameters, and calculated the transition frequencies of an impurity molecule in order to account for spectral random walk in systems such as dilute pentacene in *p*-terphenyl crystal, in which fluctuations of the transition energy arise from the flipping of the phenyl rings. The results demonstrate the large number of possible behaviors and the complexity of local impurity environments. We find that, in many cases, the power spectra of frequency fluctuations show a $1/f$ power law regardless of local configuration of spins.

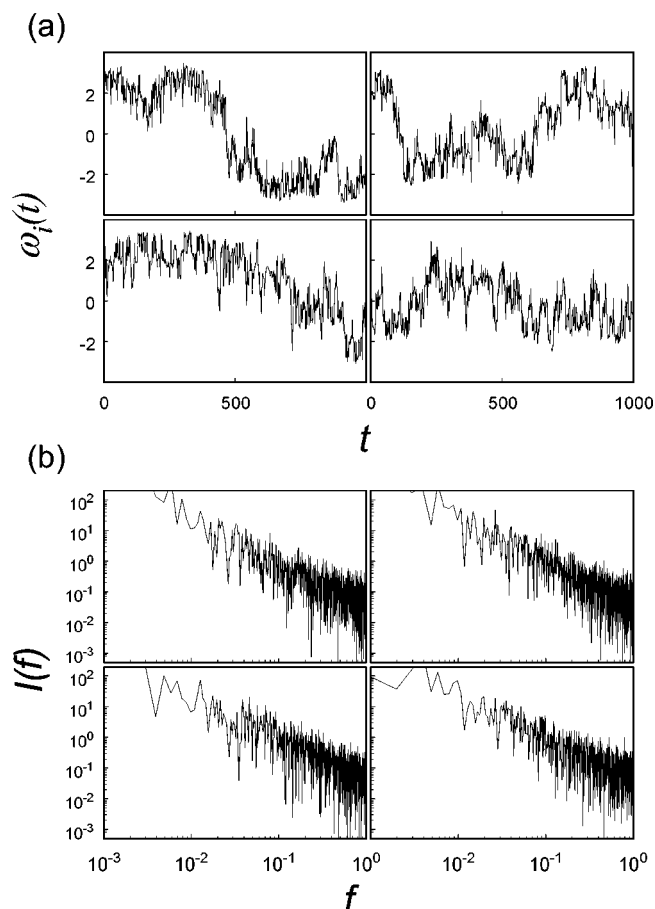


FIG. 8. Transition frequencies of impurity molecules $\omega_i(t)$ and their power spectra (log-log plot) in the case of Fig. 3(b). Each figure is placed in the same order of the impurity molecules denoted in Fig. 3(b).

The present model can be applied to study a wide range of related problems. For example, following spin glass models of water,^{38–43} one can study the dynamics of targeting molecules in water solution.

In this work, we simply study the static distribution of inhomogeneous broadening as shown in Figs. 9 and 10. The experiments on single molecule lines show that the homogeneous width measured by hole-burning or photon-echo experiments is by itself an average of a broad distribution of

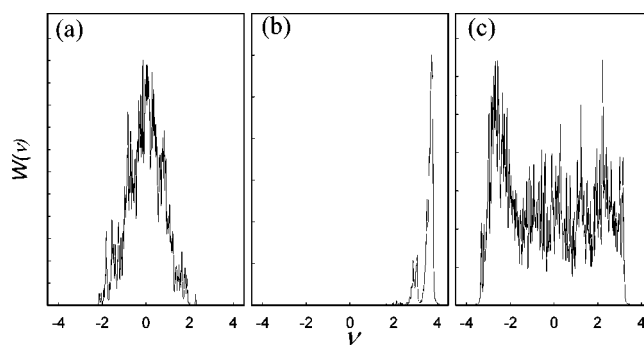


FIG. 9. Spectral distribution of $\omega_i(t)$ for Figs. 2(a)–2(c). We calculate $\omega_i(t)$ for the sites shown in Figs. 2(a)–2(c) (in each case 1024 sites) and then obtain the distribution from Eq. (3.2).

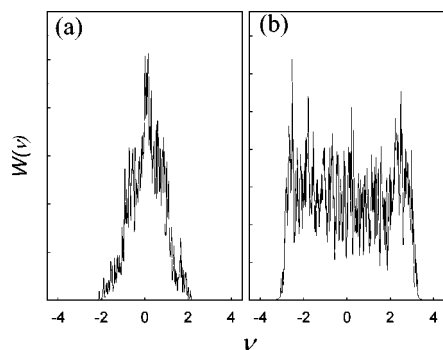


FIG. 10. Spectral distribution of $\omega_i(t)$ for Figs. 3(a)–3(b). We calculate $\omega_i(t)$ for the site shown in Figs. 3(a)–3(b) (in each case 1024 sites) and then obtain the distribution from Eq. (3.2).

widths. The model calculations that we have presented suggest that it should be possible to calculate nonlinear optical spectra in photon-echo or hole-burning experiments which may correspond to in general, non-Gaussian, situations. In addition, it allows us to explore the possibility to obtain information on local environments, such as size or structure of domains, as observed in Fig. 2(c), by using some nonlinear optical measurements such as the fifth-order spectroscopy.^{57–59}

ACKNOWLEDGMENTS

The authors would like to thank K. Saito for useful discussions about structures of terphenyl crystal. The present work was supported in part by a Grant-in-Aid for Scientific Research and a grant under the Japan–Israel International Scientific Research Program both from the Japan Ministry of Education, Science, Sports, and Culture.

¹W. P. Ambrose, Th. Basché, and W. E. Moerner, *J. Chem. Phys.* **95**, 7150 (1991).
²W. P. Ambrose and W. E. Moerner, *Nature (London)* **349**, 225 (1991).
³Th. Basché, W. P. Ambrose, and W. E. Moerner, *J. Opt. Soc. Am. B* **9**, 829 (1992).
⁴M. Pirotta, F. Güttler, H. Gyax, A. Renn, J. Sepiol, and U. P. Wild, *Chem. Phys. Lett.* **208**, 379 (1993).
⁵A.-M. Boiron, B. Lounis, and M. Orrit, *J. Chem. Phys.* **105**, 3969 (1996).
⁶F. Jelezko, Ph. Tamarat, B. Lounis, and M. Orrit, *J. Phys. Chem.* **100**, 13892 (1996).
⁷J. L. Skinner and W. E. Moerner, *J. Phys. Chem.* **100**, 13251 (1996).
⁸P. Tchénio, A. B. Myers, and W. E. Moerner, *J. Lumin.* **56**, 1 (1993).
⁹A. Zumbush, L. Fleury, R. Brown, J. Bernard, and M. Orrit, *Phys. Rev. Lett.* **70**, 3584 (1993).
¹⁰E. B. Shera, N. K. Seitzinger, L. M. Davis, R. A. Keller, and S. A. Soper, *Chem. Phys. Lett.* **174**, 553 (1990); S. A. Soper, E. B. Shera, J. C. Martin, J. H. Jett, J. H. Hahn, H. L. Nutter, and R. A. Keller, *Anal. Chem.* **63**, 432 (1991); S. A. Soper, L. M. Davis, and E. B. Shera, *J. Opt. Soc. Am. B* **9**, 1761 (1992); S. A. Soper, Q. L. Mattingly, and P. Vegunta, *Anal. Chem.* **65**, 740 (1993).
¹¹W. B. Whitten, J. M. Ramsey, S. Arnold, and B. V. Bronk, *Anal. Chem.* **63**, 1027 (1991).
¹²C. W. Wilkerson, Jr., P. M. Goodwin, W. P. Ambrose, J. C. Martin, and R. A. Keller, *Appl. Phys. Lett.* **62**, 2030 (1993).
¹³Y.-H. Lee, R. G. Maus, B. W. Smith, and J. D. Winefordner, *Anal. Chem.* **66**, 4142 (1994).
¹⁴R. Rigler, J. Widengren, and Ü. Mets, in *Fluorescence Spectroscopy*, edited by O. S. Wolfbeis (Springer, Berlin, 1993), Chap. 2; Ü. Mets and R. Rigler, *J. Fluores.* **4**, 259 (1994).

¹⁵S. Nie, D. T. Chiu, and R. N. Zare, *Science* **266**, 1018 (1994); *Anal. Chem.* **67**, 2849 (1995).
¹⁶L.-Q. Li and L. M. Davis, *Appl. Opt.* **34**, 3208 (1995).
¹⁷P. M. Goodwin, R. L. Affleck, W. P. Ambrose, J. H. Jett, M. E. Johnson, J. C. Martin, J. T. Petty, J. A. Schecker, M. Wu, and R. A. Keller, *Detection of Single Fluorescent Molecules in Flowing Sample Streams*, in *Computer Assisted Analytical Spectroscopy*, edited by S. D. Brown (Wiley, New York, 1996), Chap. 3; M. Wu, P. M. Goodwin, W. P. Ambrose, and R. Keller, *J. Phys. Chem.* **100**, 17406 (1996).
¹⁸F. Jelezko, B. Lounis, and M. Orrit, *J. Chem. Phys.* **107**, 1692 (1997).
¹⁹E. Betzig and R. J. Chichester, *Science* **262**, 1422 (1993).
²⁰W. P. Ambrose, P. M. Goodwin, J. C. Martin, and R. A. Keller, *Phys. Rev. Lett.* **72**, 160 (1994).
²¹X. S. Xie and R. C. Dunn, *Science* **265**, 361 (1994).
²²J. K. Trautman, J. J. Macklin, L. E. Brus, and E. Betzig, *Nature (London)* **369**, 40 (1994).
²³J. Wang and P. Wolynes, *Phys. Rev. Lett.* **74**, 4317 (1995).
²⁴(Eds), *Single Molecule Optical Detection, Imaging and Spectroscopy*, edited by T. Basché, W. E. Moerner, M. Orrit, and U. P. Wild (VCH, Weinheim, 1996).
²⁵Th. Basché, S. Kummer, and C. Bräuchle, *Chem. Phys. Lett.* **225**, 116 (1994).
²⁶U. P. Wild, M. Croci, F. Güttler, M. Pirotta, and A. Renn, *J. Lumin.* **60&61**, 1003 (1994).
²⁷M. Orrit, J. Bernard, R. Brown, L. Fleury, J. Wrachtrup, and C. von Broczyskowski, *J. Lumin.* **60&61**, 991 (1994).
²⁸L. Fleury, A. Zumbusch, M. Orrit, R. Brown, and J. Bernard, *J. Lumin.* **56**, 15 (1993).
²⁹L. Fleury, Ph. Tamarat, B. Lounis, J. Bernard, and M. Orrit, *Chem. Phys. Lett.* **236**, 87 (1995).
³⁰G. Zumofen and J. Klafter, *Chem. Phys. Lett.* **219**, 303 (1994).
³¹P. D. Reilly and J. L. Skinner, *Phys. Rev. Lett.* **71**, 4257 (1993); *J. Chem. Phys.* **102**, 1540 (1995).
³²J. L. Baudour, Y. Delugeard, and M. Sanquer, *Acta Crystallogr B* **30**, 691 (1974); J. L. Baudour, *ibid.* **47**, 935 (1991).
³³K. Saito, T. Atake, and H. Chihara, *Bull. Chem. Soc. Jpn.* **61**, 2327 (1988).
³⁴P. D. Reilly and J. L. Skinner, *J. Chem. Phys.* **101**, 959, 965 (1994).
³⁵R. Kubo, *Adv. Chem. Phys.* **15**, 101 (1969).
³⁶M. Mezard, G. Parisi, and M. A. Virasoro, *Spin Glass Theory and Beyond* (World Scientific, Singapore, 1987).
³⁷K. H. Fischer and J. A. Hertz, *Spin Glass* (Cambridge University Press, Cambridge, 1991).
³⁸G. M. Bell, *J. Phys. C* **5**, 889 (1972).
³⁹O. Weres and S. A. Rice, *J. Am. Ceram. Soc.* **94**, 8983 (1972).
⁴⁰P. D. Fleming III and J. H. Gibbs, *J. Stat. Phys.* **10**, 351 (1974).
⁴¹I. Ohmine and M. Sasai, *Prog. Theor. Phys. Suppl.* **103**, 61 (1991).
⁴²M. Sasai, *Bull. Chem. Soc. Jpn.* **66**, 3362 (1993).
⁴³M. Matsumoto and I. Ohmine, *J. Chem. Phys.* **104**, 2705 (1996).
⁴⁴R. J. Glauber, *J. Math. Phys.* **4**, 294 (1963).
⁴⁵M. Suzuki and R. Kubo, *J. Phys. Soc. Jpn.* **24**, 51 (1968).
⁴⁶*Monte Carlo Methods in Statistical Physics*, Topics in Current Physics, edited by K. Binder (Springer, Berlin, 1979), Vol. 1, Chap. 1.
⁴⁷J. L. Black and B. I. Halperin, *Phys. Rev. B* **16**, 2879 (1977).
⁴⁸S. Hunklinger and M. Schmidt, *Z. Phys. B* **54**, 93 (1984).
⁴⁹S. F. Edwards and P. W. Anderson, *J. Phys.* **5**, 965 (1975).
⁵⁰Y. Ozeki and H. Nishimori, *J. Phys. Soc. Jpn.* **56**, 1568, 2992 (1987).
⁵¹Y. Ozeki and H. Nishimori, *J. Phys. Soc. Jpn.* **56**, 3265 (1987).
⁵²D. Dhar, *Stochastic Processes: Formalism and Applications*, edited by G. S. Agarwal and D. Dattagupta (Springer, Berlin, 1983), p. 300.
⁵³A. J. Bray, *Phys. Rev. Lett.* **59**, 586 (1987); **60**, 720 (1988); *J. Phys. A* **22**, L81 (1989).
⁵⁴A. J. Bray and G. J. Rodgers, *J. Phys. C* **21**, L243 (1988); *Phys. Rev. B* **38**, 9252 (1988).
⁵⁵D. Dhar, M. Randeria, and J. P. Sethna, *Europhys. Lett.* **5**, 485 (1988).
⁵⁶M. Randeria, J. P. Sethna, and R. G. Palmer, *Phys. Rev. Lett.* **54**, 1321 (1985).
⁵⁷Y. Tanimura and S. Mukamel, *J. Chem. Phys.* **99**, 9496 (1993).
⁵⁸M. Cho and G. R. Fleming, *J. Phys. Chem.* **98**, 3478 (1994).
⁵⁹Y. Tanimura and K. Okumura, *J. Chem. Phys.* **106**, 2078 (1997).